

Article

The Inhibitive Effect of Sebacate-Modified LDH on Concrete Steel Reinforcement Corrosion

David Caballero ¹, Ruben Beltrán-Cobos ¹, Fabiano Tavares ², Manuel Cruz-Yusta ¹, Luis Sánchez Granados ¹, Mercedes Sánchez-Moreno ^{1,*} and Ivana Pavlovic ^{1,*}

¹ Departamento de Química Inorgánica, Instituto Universitario de Nanoquímica (IUNAN), Universidad de Córdoba, Campus de Rabanales, E-14014 Córdoba, Spain

² Departamento de Mecánica, Universidad de Córdoba, Campus de Rabanales, E-14014 Córdoba, Spain

* Correspondence: msmoreno@uco.es (M.S.-M.); iq2pauli@uco.es (I.P.)

Abstract: In recent decades, layered double hydroxides (LDH) have been proposed as innovative corrosion inhibitors for reinforced concrete. Their protective action is based on the ability to intercalate specific anions in the interlayer and on their ability to exchange the intercalated anion. In the present study, an organically charged LDH, with sebacate anions in the interlayer (LDH-S), is proposed as a water-repellent additive for mortar. The waterproofing efficiency of LDH-S and the associated corrosion inhibition ability has been evaluated in reinforced mortar samples. A 42% decrease in the water capillary absorption coefficient has been estimated when 3% LDH-S is added to a mortar. Both the passivation processes of the steel rebars during the curing period and the initiation of corrosion due to chloride exposure have been studied by electrochemical measurements. Three different mortars have been evaluated: reference mortar (REF), mortar with Mg-Al LDH (LDH), and mortar with LDH-sebacate (LDH-S). The latter has shown an important protective capacity for preventing the initiation of corrosion by chloride penetration, with an inhibitory efficiency of 74%. The presence of LDHs without sebacate in the interlayer also improved the performance of the mortar against rebar corrosion, but with lower efficiency (23% inhibitory efficiency). However, this protection is lost after continued chloride exposure over time, and corrosion initiates similarly to the reference mortar. The low corrosion current density values registered when LDH-S is added to the mortar may be related to the increased electrical resistance recorded in this mortar.

Keywords: LDH-sebacate; corrosion protection; waterproofed reinforced mortar; electrochemical measurements; capillary absorption



Citation: Caballero, D.; Beltrán-Cobos, R.; Tavares, F.; Cruz-Yusta, M.; Granados, L.S.; Sánchez-Moreno, M.; Pavlovic, I. The Inhibitive Effect of Sebacate-Modified LDH on Concrete Steel Reinforcement Corrosion. *ChemEngineering* **2022**, *6*, 72. <https://doi.org/10.3390/chemengineering6050072>

Academic Editors: Miguel A. Vicente, Raquel Trujillano and Francisco Martín Labajos

Received: 22 July 2022

Accepted: 14 September 2022

Published: 20 September 2022

Publisher's Note: MDPI stays neutral with regard to jurisdictional claims in published maps and institutional affiliations.



Copyright: © 2022 by the authors. Licensee MDPI, Basel, Switzerland. This article is an open access article distributed under the terms and conditions of the Creative Commons Attribution (CC BY) license (<https://creativecommons.org/licenses/by/4.0/>).

1. Introduction

One of the main causes of reinforced concrete deterioration in marine environments is the corrosion of the embedded rebars caused by the action of chloride ions, which reach the steel–concrete interface through the pore network of the concrete [1,2]. Generally, the steel rebars in concrete are passivated due to the high alkaline pH of the aqueous phase. However, if chloride ions reach the steel surface in sufficient concentration, the local rupture of the protective passive layer occurs, and a pitting corrosion process is initiated [3].

A first approach to solve this problem would be to prevent the entry of aggressive species into the cementitious matrix by improving the waterproofing efficiency of concrete [4]. External surface treatments are often suggested for developing waterproof concrete [5]. Different types of inorganic surface treatments have been proposed for improving concrete durability [6], such as surface coatings forming a physical barrier on the concrete surface [7], pore-blocking surface treatments that block capillary pores in concrete surface [8], and hydrophobic impregnations that inhibit water penetration [9].

The performance of surface treatments depends on the initial moisture content and the exposure environments [10]. In addition, surface treatments can degenerate over time, thus

decreasing their effectiveness [11]. In this sense, the effectiveness of the concrete waterproofing can be improved by incorporating waterproofing and/or water-repellent agents during the preparation of the mixture, which are distributed in the bulk material. Among the best-known admixtures for waterproofing concrete are crystalline admixtures [12,13], commercial compounds whose composition is not revealed by the supplier.

Layered double hydroxides (LDH) are a class of well-known crystalline compounds, commonly referred to as hydrotalcite-like compounds, because hydrotalcite (HT) is the most studied and representative mineral of this family of compounds. The HT structure can be derived from brucite-like layers, where some of the divalent cations are isomorphically substituted by trivalent ones, and the positive charge generated is balanced by intercalation of hydrated anions between the metal hydroxide layers. LDH can be represented by the general formula $[M^{2+}_{1-x}M^{3+}_x(OH)_2]^{x+}A^{n-}_{x/n} \cdot mH_2O$, where M^{2+} and M^{3+} are the divalent and the trivalent metals, and A^{n-} is the anion placed in the LDH interlayer, and is easily substitutable with others present in the aqueous solution [14]. Anions can range from simple inorganic species to complex organic anions, thus changing the interlayer LDH surface from hydrophilic to hydrophobic [14,15].

In the recent years, LDHs have been proposed as corrosion inhibitors of concrete steel reinforcements [16,17]. Both inorganic corrosion inhibitors such as nitrite [18–20] and organic corrosion inhibitors such as benzoate [21], aminobenzoate [22] or phthalate [23] have been intercalated in LDHs of different composition, Mg-Al-LDH [18–20], Ca-Al-LDH [24,25] and Zn-Al-LDH [26]. The corrosion-protective activity of LDHs is based on their ability for ionic exchange: aggressive ions, such as chloride and/or carbonate, can be adsorbed from the aqueous solution in the LDH interlayer, which can then release the corrosion inhibitors [27]. However, efficiency in the long-term of these “smart” corrosion inhibitors could fail, as the chloride trapped in the LDH could be released again [16].

A different way to protect steel rebars from corrosion in concrete is by using waterproofing concrete that prevents the entrance of water, followed by the penetration of the dissolved aggressive ions. Fatty acids are hydrophobic compounds due to the presence of hydrophobic alkyl chains. However, they have been shown to highly affect the properties of cement when added to cement-based materials in a dosage above 0.5% in clinker weight, promoting a significant increase of the setting time [28]. Nevertheless, fatty acids incorporated in the inorganic LDH matrix could be a promising additive for the waterproofing of concrete. A recent study has shown that the presence of ZnAl-LDH intercalated with the sebacate anion (ZnAl-S) in epoxy coatings significantly improves their anticorrosive properties, depending on the degree of its dispersion in the matrix [29].

The present work aimed to explore the waterproofing ability of MgAl-LDH intercalated by sebacate (LDH-S), as well as its protective capacity when added in cementitious mortars as corrosion inhibitors in the presence of chloride ions. The LDH-S was synthesized by the coprecipitation method and characterized by different techniques, such as XRD, FT-IR, TGA and ICP. The water repellent capacity of the mortar containing the LDH-S was assessed by water capillary absorption tests. The corrosion protection ability was monitored by electrochemical measurements considering two stages: the rebar passivation in the alkaline environment of the mortar, and the corrosion initiation due to the chloride penetration through the mortar pores.

2. Materials and Methods

$Mg(NO_3)_2 \cdot 6H_2O$, $Al(NO_3)_3 \cdot 9H_2O$ and sebacic acid $((CH_2)_8(COOH)_2)$ were acquired from Sigma-Aldrich (St. Louis, MO, USA). All of the chemicals were at least 98–99%. Portland CEM II/A-L 42.5 R from Cosmos Cements, siliceous sand with a maximum size of 1.5 mm and tap water were used as raw materials for preparing the mortar samples.

2.1. Synthesis of LDH

Organic LDH, LDH-S, was obtained through the coprecipitation method in a N_2 atmosphere and using CO_2 -free water, adding 250 mL of solution containing 0.15 mol of

$\text{Mg}(\text{NO}_3)_2 \cdot 6\text{H}_2\text{O}$ and 0.05 mol of $\text{Al}(\text{NO}_3)_3 \cdot 9\text{H}_2\text{O}$ to 500 mL of the alkaline (0.16 mol of NaOH) 0.125 mol sebacate solution. The LDH suspensions thus obtained were filtered and washed with CO_2 -free, distilled water and dried at 60 °C. For comparison purposes, a MgAl-CO_3 (LDH- CO_3) was prepared with the coprecipitation method, dropping a solution containing 0.75 mol of $\text{Mg}(\text{NO}_3)_2 \cdot 6\text{H}_2\text{O}$ and 0.25 mol of $\text{Al}(\text{NO}_3)_3 \cdot 9\text{H}_2\text{O}$ into a solution containing 1.7 mol of NaOH and 0.5 mol of Na_2CO_3 . The resultant suspension was washed with distilled water and dried at 60 °C.

2.2. Characterization of LDH Additives

X-ray diffraction (XRD) patterns were recorded by a Bruker D8 Discover diffractometer (Bruker, Karlsruhe, Germany). The Fourier transform infrared spectra (FT-IR) were recorded by PerkinElmer Frontier MIR using ATR (PerkinElmer España SL, Madrid, Spain).

Elemental chemical analyses were measured by Induced Coupled Plasma mass spectroscopy (ICP-MS) on a PerkinElmer Nexion-X instrument (PerkinElmer España SL, Madrid, Spain).

2.3. Production of Mortar Samples for Water Capillary Absorption Tests

Cylindrical specimens of 70 mm in diameter and 30 mm in height were manufactured for the water capillary absorption test. A cement/sand/water dosage of 1/3/0.5 was used for producing the cementitious mortar. Mortars incorporating additives were mixed with 3% by cement weight of the LDH. Both LDHs (LDH-S and LDH- CO_3) were considered.

Mortar samples were demolded 24 h after casting and cured under controlled climate conditions at 21 ± 2 °C and >95% HR. Two samples of each mortar were evaluated for repeatability assessment.

2.4. Production of Reinforced Mortar Samples

Reinforced mortar specimens were prepared by embedding steel rebars 500S (6 mm nominal diameter) in a mortar cover of approximately 1 cm. A mortar with similar composition to the one used for the waterproofing test was used in the reinforced specimens. Mortars incorporating LDH-based additives (M-LDH-S and M-LDH- CO_3) in 3% by cement weight were also studied.

The exposed area of the bars was delimited to 6 cm² covering the edge of the bar with isolating tape. Before embedding in mortar, steel rebars were cleaned in a HCl:H₂O 1:1 with 5 g/L urotropine solution and degreased in acetone. The final aspect of the steel rebar before testing is shown in Figure 1 (left). Two rebars were tested for each mortar for repeatability assessment.

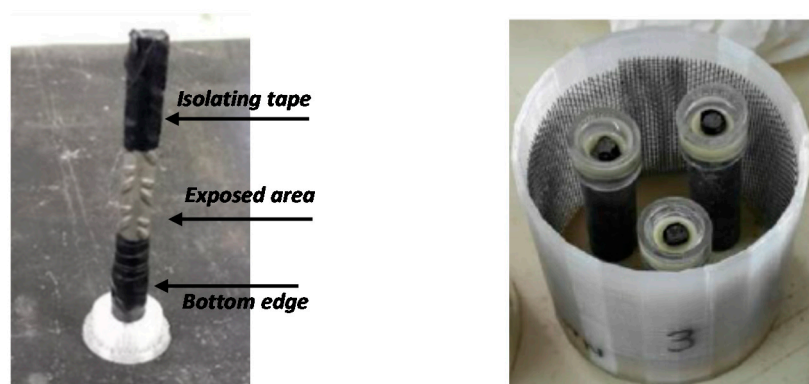


Figure 1. (Left)—Rebar before embedding in mortar. (Right)—Electrochemical cell with three reinforced mortar samples and the stainless-steel mesh used as a counter-electrode for the electrochemical tests.

Reinforced samples were demolded 24 h after casting, and immersed in an alkaline solution of $\text{Ca}(\text{OH})_2$ for curing. After 28 days curing in the alkaline conditions, the alkaline

solution was changed by a 0.5 M NaCl solution for 50 days. In this way, both the passivation and the corrosion stages could be monitored by periodic electrochemical measurements.

2.5. Waterproofing Efficiency of the LDH-Based Additives

The waterproofing efficiency of the studied mortars was assessed after 14 days curing. Measurements were carried out for 3 days according to the Fagerlund method [30]. The mortar specimens were placed 5 mm in contact with water and periodically weighed. From the weight–time curve obtained, two parameters can be deduced: the saturation time, when the weight gain is stabilized, and the water capillary absorption coefficient, estimated according to [30]. For each type of studied mortar, the average value of the two tested samples was considered.

2.6. Electrochemical Tests

A three-electrode electrochemical cell was used for monitoring the corrosion response of the steel rebars, as shown in Figure 1 (right). For the electrochemical measurements, a stainless-steel mesh located around the samples was used as a counter-electrode, an Ag/AgCl electrode in 3 M KCl was used as a reference electrode, and the reinforced samples acted as working electrodes.

An Autolab PGSTAT204 potentiostat/galvanostat with a frequency analyzer module (FRA) using NOVA software was used for the electrochemical tests. The evolution of the corrosion potential (E_{corr}), the electrical resistance of the mortar cover (R_e) and the polarization resistance (R_p) of the steel rebars were periodically measured. R_p values were obtained by linear potential sweep from -10 mV to $+10$ mV with respect to the measured corrosion potential. R_e was determined by applying an alternating current at a single frequency of 1000 Hz between the rebar and the counter electrode. A potentiostatic method with an amplitude of 10 mV_{rms} around E_{corr} was defined.

Electrochemical measurements were considered only after 4 days curing of the mortars, before non-stable response of the different parameters monitored were registered.

At the end of the test, to accelerate the corrosion process and make the chloride-generated pitting more visible, a constant potential of $+250$ mV vs. Ag/AgCl reference electrode was applied for 4 h.

The corrosion current density (i_{corr}) was obtained indirectly using the Stern and Geary equation [31], $i_{corr} = \frac{B}{R_p \cdot A}$, where B is a constant equal to 26 mV [32], R_p is the value of polarization resistance, and A is the exposed area. The inhibitory efficiency of the LDH was estimated at the end of the test using the following equation:

$$EI(\%) = \frac{i_{acum, REF} - i_{acum, LDH}}{i_{acum, REF}} \cdot 100 \quad (1)$$

where $i_{acum, REF}$ and $i_{acum, LDH}$ are the cumulative values of corrosion current density during the whole test for the reference mortar, and the mortars with LDH, respectively.

3. Results and Discussion

3.1. Characterization of the LDH Additives

The diffraction patterns of both additives, included in Figure 2, were characteristic of LDH compounds, with intense basal reflections (00 l) at low angles and low asymmetric reflections at intermediate and high angles [14,15]. An increase in d (003) value for the LDH-S was observed compared to LDH-CO₃ (15.6 Å for LDH-S vs. 7.8 Å for LDH-CO₃), as expected due to the larger size of sebacate anion and in agreement with [29,33].

Although we carried out a very careful synthesis under inert conditions, the reflection at 24° in 2 θ indicates that the LDH-S sample mixed with sebacate also contained a certain amount of carbonate, since this anion has a very high affinity for the intermediate layer. The position of the (012) plane characteristic for LDH compounds, which overlaps with the (009) reflection for LDH-CO₃, was maintained unchanged in the HT-S sample pattern [14,34].

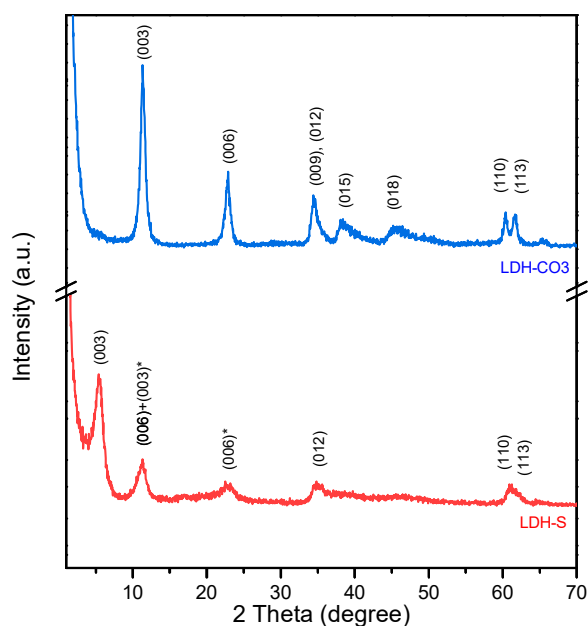


Figure 2. XRD patterns of LDH-CO₃ and LDH-S. * Peaks of the carbonate phase in LDH-S.

The FT-IR spectra of LDH-CO₃ (Figure 3) shows a characteristic band at around 3500 cm⁻¹, corresponding to the water molecules and free OH⁻ groups stretching vibrations, the band at 1650 cm⁻¹ corresponding to the bending mode vibration of water molecules, and the band at 1375 cm⁻¹ of the carbonate antisymmetrical stretching mode. LDH-S spectra showed the most characteristic bands of fatty acid at around 1560 cm⁻¹ and 1460 cm⁻¹ due to antisymmetrical and symmetrical vibrations of carboxylate groups, respectively, as well as the C-H stretching vibrations at ~2900 cm⁻¹ and bending vibrations at ~1408 cm⁻¹ of the aliphatic chains. The absence of the protonated carboxylic group (-COOH) band of sebacic acid at ~1700 cm⁻¹ confirmed that this compound is intercalated in the interlayer in its anionic form.

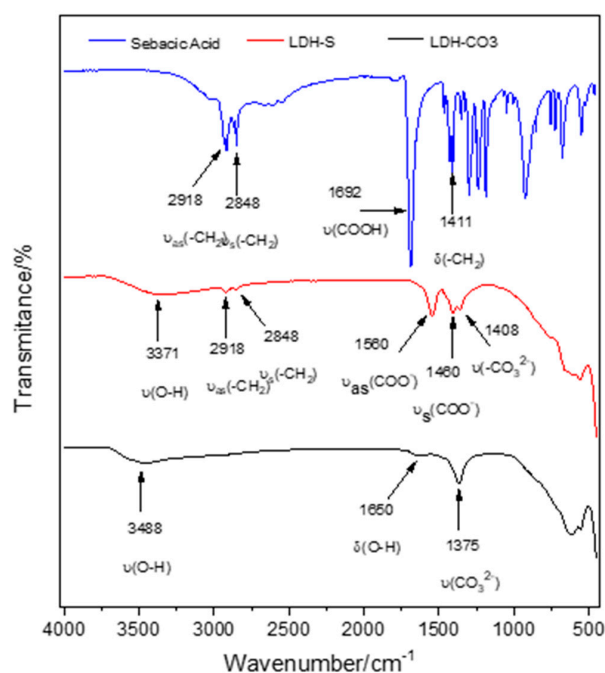


Figure 3. FT-IR spectra patterns of LDH-CO₃ and LDH-S.

These findings, in agreement with XRD results (Figure 2), corroborate the intercalation of sebacate anions in the LDH interlayer.

3.2. Water Capillary Absorption Test

In Figure 4, the weight gain as function of the square root of time for the three tested mortars is represented (the average value of two samples per mortar is shown). Typical behavior can be observed in two different stages: during the first hours, a linear weight increase with the time is registered, until the second stage is reached, in which the weight gain is almost stabilized.

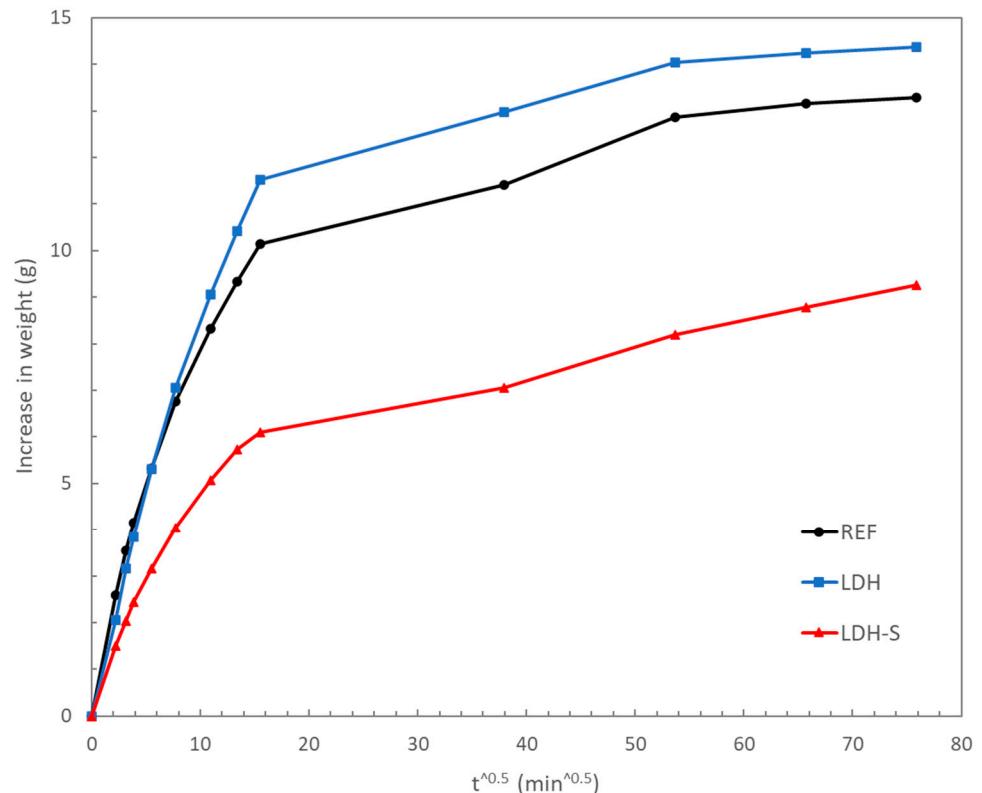


Figure 4. Water capillary absorption tests in mortars after 14 days curing.

In the case of the mortar with waterproofing additive (M-LDH-S), a significant decrease was observed both in the rate of water penetration during the first hours and in the total amount of water absorbed. However, in the case of mortars with LDH-CO₃, similar behavior to the case of the reference was observed. The time of saturation (t_n) estimated of all the studied mortars (between 3–4 h) was as detailed in Table 1. The water capillary absorption coefficient (K), estimated according to [30], is detailed in Table 1 for the different studied mortars.

Table 1. Water capillary absorption coefficients estimated according to the Fagerlund method [30].

Sample	t_n (min)	K (kg/cm ² min ^{0.5})
M-REF	208	0.0184
M-LDH-CO ₃	190	0.0220
M-LDH-S	224	0.0104

An increase in the saturation time and a decrease in the water capillary absorption coefficient was obtained in the case of mortar incorporating LDH-S. A waterproofing efficiency of 42% can be estimated from the K values included in Table 1. When LDH-CO₃

was added to the mortar, no improvement in water penetration by capillary absorption was observed. In fact, even higher values of K were obtained in this case.

3.3. Passivation Stage of Reinforced Mortars

The passivation of the steel rebars embedded in the mortars was monitored during the curing period by monitoring the evolution of the corrosion potential, and the corrosion current density estimated by the Stern-Geary equation, as described in the previous section. In each studied mortar, the two rebars showed a similar evolution, and thus, in the results of the present study, the mean value between two rebars is used.

In Figure 5, the evolution of the corrosion potential (E_{corr}) for the three studied mortars is represented. The typical passivation process, with a continuous increase of the potential during the first days of rebar contact with the alkaline phase of the mortar pores, was registered. After about 15 days curing, the three studied mortars showed values of E_{corr} above -0.2 V vs. SCE, that is, the criteria established by Rilem Recommendations [35] as a low probability for active corrosion occurring.

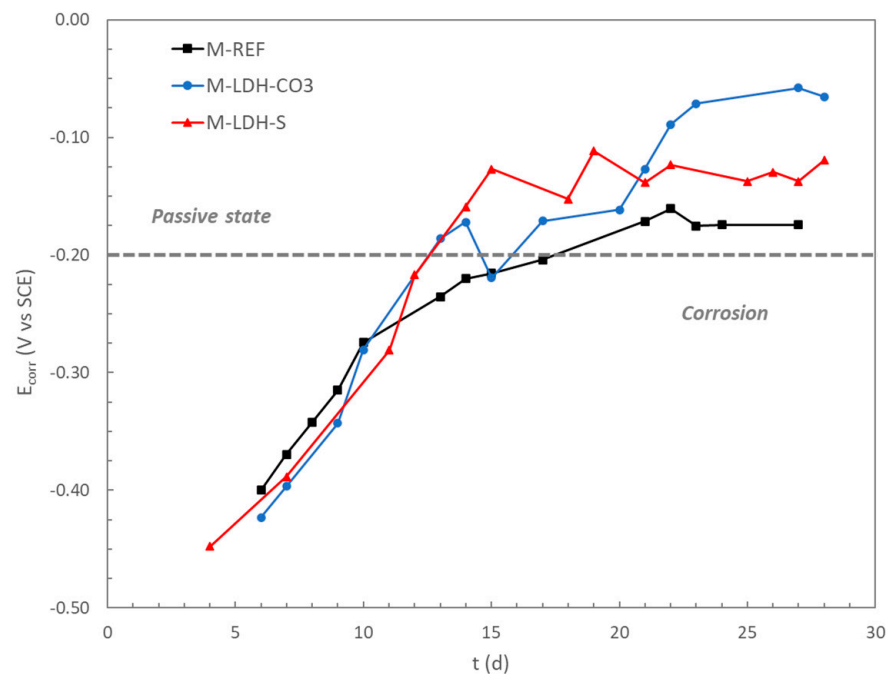


Figure 5. Evolution of the corrosion potential for the three studied reinforced mortars during the passivation stage.

Concerning the evolution of the corrosion current density (i_{corr}), the typical response of a passivation process was also observed for the three studied mortars, as shown in Figure 6. In this case, lower values of i_{corr} during the whole period of curing were registered for the rebars embedded in mortar containing LDH-S. The inhibitive action of the sebacate incorporated in the interlayer of the LDH can be confirmed when compared to the evolution of i_{corr} for the rebars in mortars with LDH-CO₃. In this latter case, higher corrosion rates were registered, as well as a delay in reaching the corrosion values below $0.2 \mu\text{A}/\text{cm}^2$, which can be considered as the boundary between negligible and active moderate corrosion [36]. The presence of sebacate in the interlayer of the LDH seems to promote the passivation of the rebar, as the passive situation related to a negligible corrosion was reached before the reference case, and lower i_{corr} values were maintained.

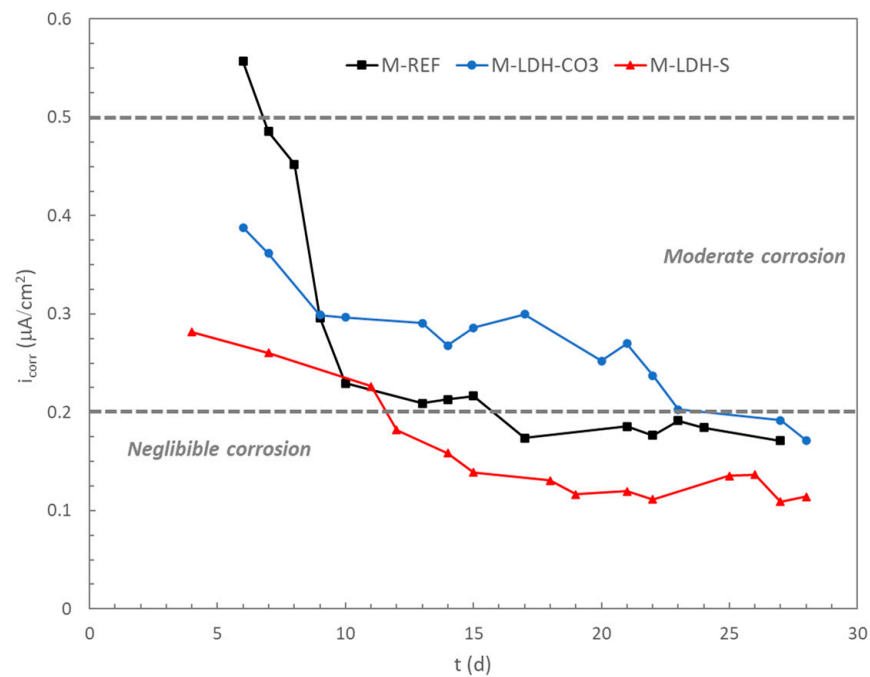


Figure 6. Evolution of the corrosion current density for the three studied reinforced mortars during the passivation stage.

The electrical resistance of the mortar cover was also monitored during the entire passivation period, as shown in Figure 7.

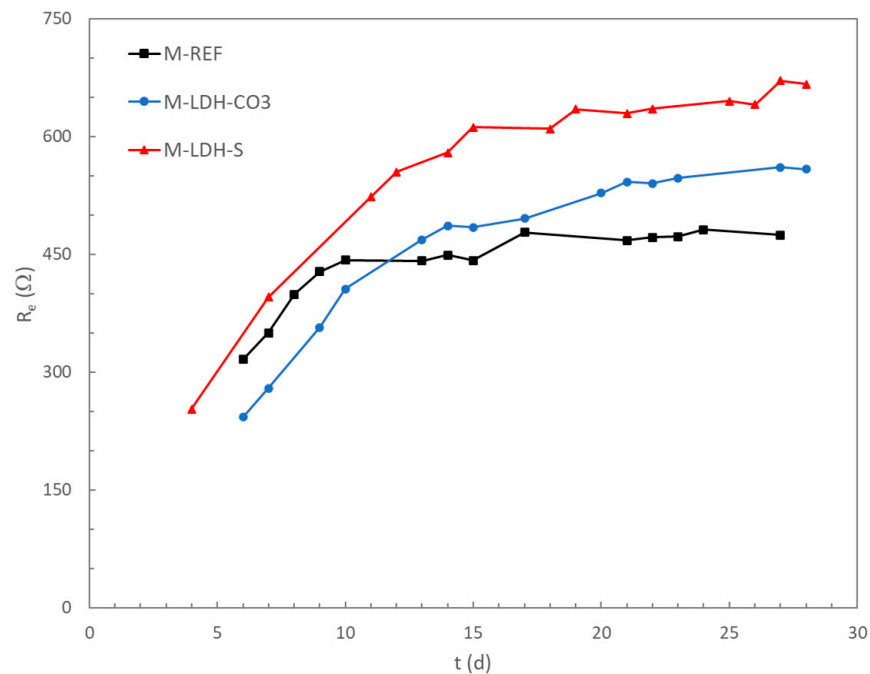


Figure 7. Evolution of the electrical resistance for the three studied reinforced mortars during the passivation period.

A continuous increase during the first days of curing was observed in all the mortars, as expected due to the evolution of the hydrated solid phases in the cementitious matrix. After some time, an almost constant value of the electrical resistance was reached for the different mortars. This steady stage was reached faster in the case of the reference mortar

without any additive than in the other mortars, probably due to the continuous release of water from the LDH that promotes later hydration processes of the cementitious matrix [37]. Higher values of the electrical resistance were measured for the M-LDH-S, as expected due to the water-repellent ability of this additive, as has been confirmed in Section 3.2 in the present study. The higher values of the electrical resistance in the mortar incorporating LDH-S seem to be related to a more protective action of this mortar on the passivation processes of the steel rebars (see Figure 6).

3.4. Corrosion Stage of Reinforced Mortars

As detailed in the previous section, after the passivation of the rebars during the curing period in saturated calcium hydroxide, the reinforced samples were exposed to a chloride solution to promote the penetration of the chloride ions through the concrete pores to the rebar. During this stage, the same electrochemical parameters as in the passivation stage were monitored: corrosion potential (E_{corr}) and corrosion current density (i_{corr}).

In Figure 8, the evolution of the corrosion potential during the exposure to chloride penetration is shown. A rapid significant decrease of the corrosion potential in all cases can be observed after just the first day of immersion of the reinforced mortar samples in the solution of sodium chloride.

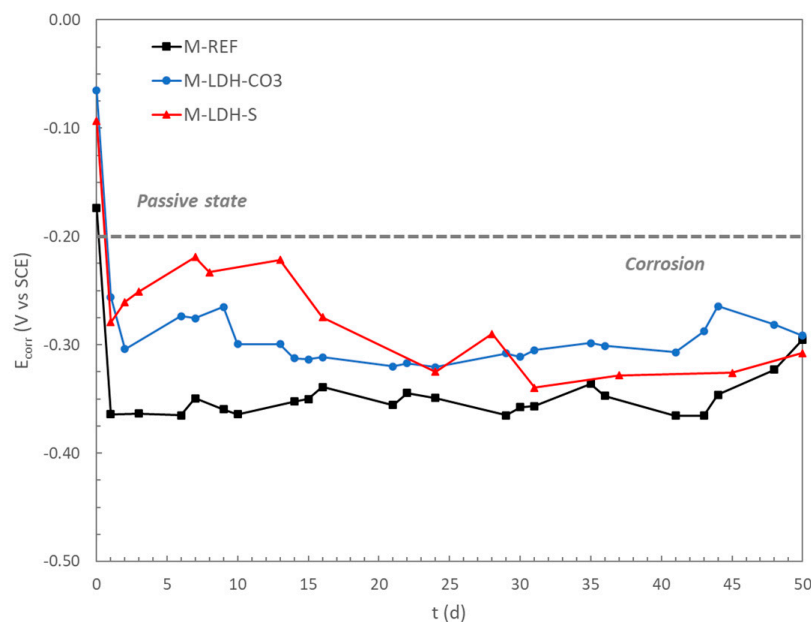


Figure 8. Evolution of the corrosion potential for the three studied reinforced mortars during the corrosion stage (exposure to chloride action).

In the case of the reference mortar, the drop in potential was higher than in the case of the mortar with LDH additives. The potential decrease in the mortar with LDH-S was less significant, and only in this case the E_{corr} seemed to evolve to more anodic values during the first days of exposure to the chloride solution.

When the corrosion current density evolution is considered, the behavior of the three studied reinforced mortars was different during the exposure to chloride action, as can be observed from Figure 9.

In the case of the reference sample, an increase of i_{corr} values to the region considered as moderate corrosion ($>0.2 \mu\text{A}/\text{cm}^2$) was registered after 7 days of exposure to the chloride penetration, indicating the corrosion initiation of the embedded rebars. In the mortar with LDH- CO_3 , this increase occurred after approximately 25 days of chloride exposure, probably due to the ability of LDH to trap chloride. In fact, the i_{corr} values fluctuated on the limit between passivation and corrosion for a few days, until a new increase of i_{corr} values was produced after 40 days of exposure to chloride action.

When LDH-S was added to the mortar, rebars did not show any sign of corrosion even after 50 days of exposure to chloride, confirming the protective ability of the LDH-S as a corrosion inhibitor. Low values of i_{corr} , below $0.1 \mu\text{A}/\text{cm}^2$, were maintained during the whole test.

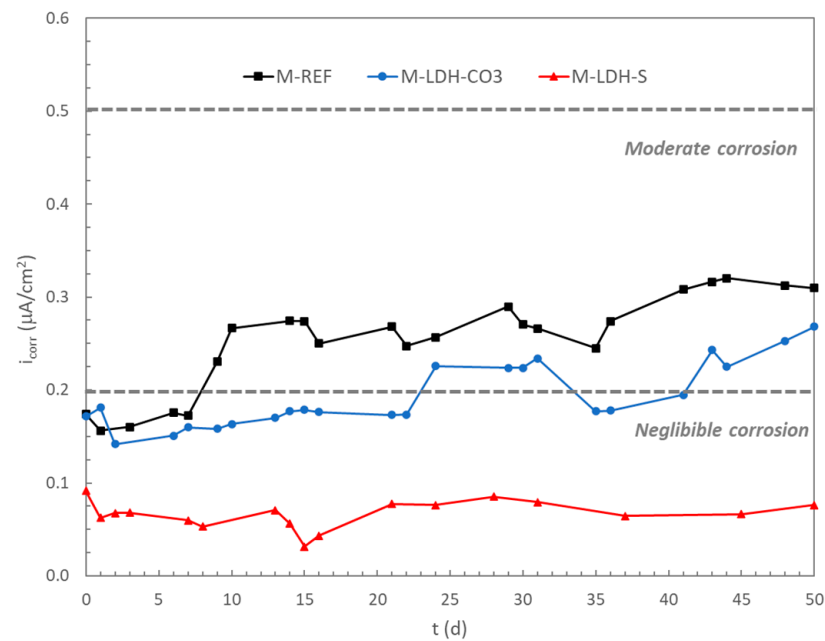


Figure 9. Evolution of the corrosion current density for the three studied reinforced mortars during the corrosion stage (exposure to chloride action).

3.5. Inhibitory Efficiency of LDH-Based Additives

To evaluate the efficiency of the corrosion inhibitors based on LDH, the total charge passed during the entire chloride exposure period (Q_{corr}) has been estimated and represented in Figure 10 for the different studied mortars. In this case, the response of each rebar has been considered, and therefore two points for each mortar are shown in Figure 10.

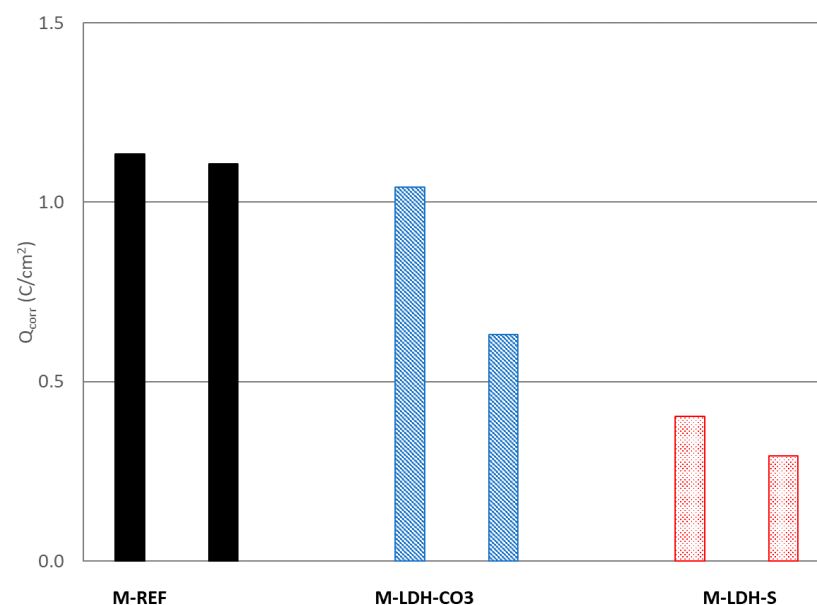


Figure 10. Total charge associated with the corrosion period (exposure to chloride action) for each studied rebar.

While in the case of M-REF and M-LDH-S, a similar response is registered for the two embedded rebars in each case, in the case of M-LDH-CO₃, higher variability is observed. Nevertheless, it can be observed that both M-LDH-CO₃ and M-LDH-S showed lower values of charge, indicating a certain higher protective ability of these mortars. When LDH-S was added to the mortar, the decrease was significantly higher, confirming the higher efficiency of this additive as a corrosion inhibitor. The inhibitory efficiency of both additives can be estimated using Equation (1), and the mean values of 74% and 23% were obtained for M-LDH-S and M-LDH-CO₃, respectively.

At the end of the chloride exposure, one rebar of each mortar was subjected to an anodic current by connecting the rebar to +0.250 V vs. SCE for 4 h to accelerate the corrosive development, making the damage more visible to visual inspection of the rebars. In Figure 11, the photographs of the exposed surface after the anodic polarization are included.

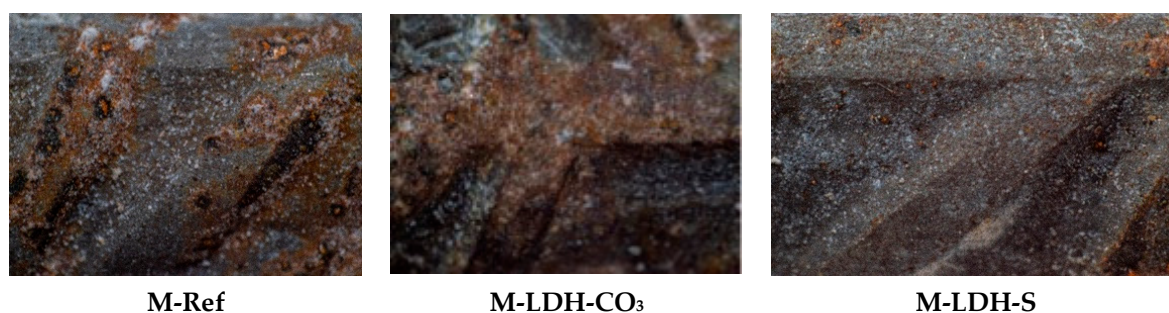


Figure 11. Visual aspect of the rebars at the end of the test.

The visual inspection of the rebar surface confirms the electrochemical results. While the reference mortar and the M-LDH-CO₃ show corrosion spots distributed on the exposed surface, in the case of the M-LDH-S mortar, the presence of these spots is not evident.

4. Conclusions

The waterproofing ability of LDH with sebacate (LDH-S) in the interlayer has been confirmed with a decrease of 42% in the water capillary absorption coefficient. This water-repellent capacity resulted in a very effective corrosion inhibition for steel rebars embedded in mortar with 3% LDH-S (74% inhibition). The effect of LDH-S can be observed from the passivation of the rebar due to the contact with the alkaline aqueous phase of mortar pores. The action of LDH-S seems to be related to the increase in the electrical resistance values of the mortar cover due to the hydrophobic effect caused by sebacate presence.

A less effective corrosion inhibition, associated with the presence of LDH in the mortar, has been also observed (23% inhibition), probably due to the ability of this additive to trap chloride ions. However, this protection was lost after continued chloride exposure, and corrosion initiated similarly to the reference mortar.

Further studies are underway to analyze the protection mechanism associated to the presence of LDH-S in the mortar.

Author Contributions: Conceptualization, M.C.-Y., L.S.G., M.S.-M. and I.P.; methodology, D.C., R.B.-C., F.T. and M.S.-M.; software, R.B.-C. and F.T.; validation, M.C.-Y., L.S.G., M.S.-M. and I.P.; formal analysis, D.C., M.S.-M. and I.P.; investigation, D.C., L.S.G., M.S.-M. and I.P.; resources, F.T., L.S.G., M.S.-M. and I.P.; data curation, M.S.-M. and I.P.; writing—original draft preparation, M.S.-M. and I.P.; writing—review and editing, M.C.-Y., L.S.G., M.S.-M. and I.P.; visualization, M.C.-Y., L.S.G., M.S.-M. and I.P.; supervision, L.S.G., M.S.-M. and I.P.; project administration, L.S.G. and M.S.-M.; funding acquisition, M.C.-Y., L.S.G., M.S.-M. and I.P. All authors have read and agreed to the published version of the manuscript.

Funding: This research was 80% funded by P.O. FEDER Andalucía (2014–2020)/Consejería de Transformación Económica, Industria, Conocimiento y Universidad/_Proyecto Ref. PY20_00365 “Incorporación de compuestos tipo hidrotalcita (HDL) en tratamientos superficiales multifuncionales para la reparación de infraestructuras de hormigón”.

Data Availability Statement: Data can be found on the Zenodo platform (10.5281/zenodo.7092247).

Acknowledgments: The authors thank Cementos Cosmos S.A. for supplying the cement for manufacturing the mortar specimens.

Conflicts of Interest: The authors declare no conflict of interest.

References

1. Alonso, C.; Andrade, C.; Castellote, M.; Castro, P. Chloride threshold values to depassivate reinforcing bars embedded in a standardized OPC mortar. *Cem. Concr. Res.* **2000**, *30*, 1047–1055. [[CrossRef](#)]
2. Yuan, Q.; Shi, C.; De Schutter, G.; Audenaert, K.; Deng, D. Chloride binding of cement-based materials subjected to external chloride environment—A review. *Constr. Build. Mater.* **2009**, *23*, 1–13. [[CrossRef](#)]
3. Saremi, M.; Mahallati, E. A study on chloride-induced depassivation of mild steel in simulated concrete pore solution. *Cem. Concr. Res.* **2002**, *32*, 1915–1921. [[CrossRef](#)]
4. Muhammad, N.Z.; Keyvanfar, A.; Mamjid, M.Z.A.; Shafaghat, A.; Mirza, J. Waterproof performance of concrete: A critical review on implemented approaches. *Constr. Build. Mater.* **2015**, *101*, 80–90. [[CrossRef](#)]
5. Sánchez, M.; Faria, P.; Ferrara, L.; Horszczaruk, E.; Jonkers, H.M.; Kwiecien, A.; Mosa, J.; Peled, A.; Pereira, A.S.; Snoeck, D.; et al. External treatments for the preventive repair of existing constructions: A review. *Constr. Build. Mater.* **2018**, *193*, 435–452. [[CrossRef](#)]
6. Pan, X.; Shi, Z.; Shi, C.; Ling, T.C.; Li, N. A review on concrete surface treatment Part I: Types and mechanisms. *Constr. Build. Mater.* **2017**, *132*, 578–590. [[CrossRef](#)]
7. Almusallam, A.A.; Khan, F.M.; Dulaijan, S.U.; Al-Amoudi, O.S.B. Effectiveness of surface coatings in improving concrete durability. *Cem. Concr. Compos.* **2003**, *25*, 473–481. [[CrossRef](#)]
8. Jiang, L.; Xue, X.; Zhang, W.; Yang, J.; Zhang, H.; Li, Y.; Zhang, R.; Zhang, Z.; Xu, L.; Qu, J. The investigation of factors affecting the water impermeability of inorganic sodium silicate-based concrete sealers. *Constr. Build. Mater.* **2015**, *93*, 729–736. [[CrossRef](#)]
9. Li, J.; Yi, Z.; Xie, Y. Progress of Silane Impregnating Surface Treatment Technology of Concrete Structure. *Mater. Rev.* **2012**, *26*, 120–125.
10. Bao, J.; Li, S.; Zhang, P.; Xue, S.; Cui, Y.U.; Zhao, T. Influence of exposure environments and moisture content on water repellency of surface impregnation of cement-based materials. *J. Mater. Res. Technol.* **2020**, *9*, 12115–12125. [[CrossRef](#)]
11. Allahviridzadeh, R.; Reshetnia, R.; Dousti, A.; Shekarchi, M. Application of polymer concrete in repair of concrete structures: A literature review. In *Concrete Solutions*, 1st ed.; Grantham, M., Mechtcherine, V., Schneck, U., Eds.; CRC Press: London, UK, 2011; pp. 435–444.
12. Al-Kheetan, M.J.; Rahman, M.M.; Chamberlain, D.A. A novel approach of introducing crystalline protection material and curing agent in fresh concrete for enhancing hydrophobicity. *Constr. Build. Mater.* **2018**, *160*, 644–652. [[CrossRef](#)]
13. Al-Rashed, R.; Al-Jabari, M. Concrete protection by combined hygroscopic and hydrophilic crystallization waterproofing applied to fresh concrete. *Case Stud Constr Mater* **2021**, *15*, e00635. [[CrossRef](#)]
14. Rives, V. *Layered Double Hydroxides: Present and Future*; Nova Science Publishers, Inc.: New York, NY, USA, 2001.
15. Cavani, F.; Trifirò, F.; Vaccari, A. Hydrotalcite-type anionic clays: Preparation, properties and applications. *Catal. Today* **1991**, *11*, 173–301. [[CrossRef](#)]
16. Yang, H.; Xiong, C.; Liu, X.; Liu, A.; Li, T.; Ding, R.; Shah, S.P.; Li, W. Application of layered double hydroxides (LDHs) in corrosion resistance of reinforced concrete—State of the art. *Constr. Build. Mater.* **2021**, *307*, 124991. [[CrossRef](#)]
17. Mir, Z.M.; Bastos, A.; Höche, D.; Zheludkevich, M. Recent Advances on the Application of Layered Double Hydroxides in Concrete—A Review. *Materials* **2020**, *13*, 1426. [[CrossRef](#)]
18. Cao, Y.; Dong, S.; Zheng, D.; Wang, J.; Zhang, X.; Du, R.; Song, G.; Lin, C. Multifunctional inhibition based on layered double hydroxides to comprehensively control corrosion of carbon steel in concrete. *Corros. Sci.* **2017**, *126*, 166–179. [[CrossRef](#)]
19. Zuo, J.; Wu, B.; Luo, C.; Dong, B.; Xing, F. Preparation of MgAl layered double hydroxides intercalated with nitrite ions and corrosion protection of steel bars in simulated carbonated concrete pore solution. *Corros. Sci.* **2019**, *152*, 120–129. [[CrossRef](#)]
20. Ma, G.; Xu, J.; Han, L.; Xu, Y. Enhanced inhibition performance of NO₂⁻ intercalated MgAl-LDH modified with nano-SiO₂ on steel corrosion in simulated concrete pore solution. *Corros. Sci.* **2022**, *204*, 110387. [[CrossRef](#)]
21. Wu, B.; Zuo, J.; Dong, B.; Xing, F.; Luo, C. Study on the affinity sequence between inhibitor ions and chloride ions in Mg-Al layer double hydroxides and their effects on corrosion protection for carbon steel. *Appl. Clay Sci.* **2019**, *180*, 105181. [[CrossRef](#)]
22. Yang, Z.; Fischer, H.; Cerezo, J.; Mol, J.M.C.; Polder, R. Modified hydrotalcites for improved corrosion protection of reinforcing steel in concrete—Preparation, characterization, and assessment in alkaline chloride solution. *Mater. Corros.* **2016**, *71*, 721–738. [[CrossRef](#)]

23. Cao, Y.; Zheng, D.; Dong, S.; Zhang, F.; Lin, J.; Wang, C.; Lin, C. A Composite Corrosion Inhibitor of MgAl Layered Double Hydroxides Co-Intercalated with Hydroxide and Organic anions for Carbon Steel in Simulated Carbonated Concrete Pore Solutions. *J. Electrochem. Soc.* **2019**, *166*, C3106–C3113. [[CrossRef](#)]
24. Chen, Y.; Shui, Z.; Chen, W.; Chen, G. Chloride binding of synthetic Ca-Al-NO₃ LDHs in hardened cement paste. *Constr. Build. Mater.* **2015**, *93*, 1051–1058. [[CrossRef](#)]
25. Yang, Z.; Fischer, H.; Polder, R. Synthesis and characterization of modified hydrotalcites and their ion exchange characteristics in chloride-rich simulated concrete pore solution. *Cem. Concr. Compos.* **2014**, *47*, 87–93. [[CrossRef](#)]
26. Tian, Y.; Dong, C.; Wang, G.; Cheng, X.; Li, X. Zn-Al-NO₂ layered double hydroxide as a controlled-release corrosion inhibitor for steel reinforcements. *Mater. Lett.* **2019**, *236*, 517–520. [[CrossRef](#)]
27. Tian, Y.; Wen, C.; Wang, G.; Deng, P.; Mo, W. Inhibiting property of nitrite intercalated layered double hydroxide for steel reinforcement in contaminated concrete condition. *J. Appl. Electrochem.* **2020**, *50*, 835–849. [[CrossRef](#)]
28. Albayrak, A.T.; Yasar, M.; Gurkaynak, M.A.; Gurgey, I. Investigation of the effects of fatty acids on the compressive strength of the concrete and the grindability of the cement. *Cem. Concr. Res.* **2005**, *35*, 400–404. [[CrossRef](#)]
29. Nguyen, D.T.; To, H.T.X.; Gervasi, J.; Paint, Y.; Gonon, M.; Olivier, M.G. Corrosion inhibition of carbon steel by hydrotalcites modified with different organic carboxylic acids for organic coatings. *Prog. Org. Coat.* **2018**, *124*, 256–266. [[CrossRef](#)]
30. *UNE 83982:2008*; Concrete Durability. Test Methods. Determination of the Capillar Suction in Hardened Concrete; Fagerlund Method. AENOR: Madrid, Spain, 2008.
31. Stern, M.; Geary, A.L. Electrochemical polarization, I. A theoretical analysis of the shape of polarization curves. *J. Electrochem. Soc.* **1957**, *104*, 56–63. [[CrossRef](#)]
32. Andrade, C.; Maribona, I.R.; Feliu, S.; González, J.A.; Feliu, S., Jr. The effect of macrocells between active and passive areas of steel reinforcements. *Corr. Sci.* **1992**, *33*, 237–249. [[CrossRef](#)]
33. Chacara, D.; Bruna, F.; Ulibarri, M.A.; Draoui, K.; Barriga, C.; Pavlovic, I. Organo/layered double hydroxide nanohybrids used to remove non ionic pesticides. *J. Hazard. Mater.* **2011**, *196*, 350–359. [[CrossRef](#)]
34. Dietmann, K.M.; Linke, T.; Trujillano, R.; Rives, V. Effect of Chain Length and Functional Group of Organic Anions on the Retention Ability of MgAl- Layered Double Hydroxides for Chlorinated Organic Solvents. *ChemEngineering* **2019**, *3*, 89. [[CrossRef](#)]
35. Elsener, B. RILEM TC 154-EMC: Electrochemical techniques for measuring metallic corrosion—Recommendations—Half-cell potential measurements—Potential mapping on reinforced concrete structures. *Mater. Struct.* **2003**, *36*, 461–471. [[CrossRef](#)]
36. Garcés, P.; Andrade, M.C.; Saez, A.; Alonso, M.C. Corrosion of reinforcing steel in neutral and acid solutions simulating the electrolytic environments in the micropores of concrete in the propagation period. *Corros. Sci.* **2005**, *47*, 289–306. [[CrossRef](#)]
37. Shui, Z.H.; Yu, R.; Chen, Y.X.; Duan, P.; Ma, J.T.; Wang, X.P. Improvement of concrete carbonation resistance based on a structure modified layered double hydroxides (LDHs): Experiments and mechanism analysis. *Constr. Build. Mater.* **2018**, *176*, 228–240. [[CrossRef](#)]